Computer Methods and Programs in Biomedicine 243 (2024) 107935

Contents lists available at ScienceDirect

Computer Methods and Programs in Biomedicine

journal homepage: www.elsevier.com/locate/cmpb

SGABU computational platform for multiscale modeling: Bridging the gap between education and research

Tijana Geroski [a,b,*], Orestis Gkaintes [c], Aleksandra Vulović [a,b], Niketa Ukaj [d], Jorge Barrasa-Fano [e], Fernando Perez-Boerema [e], Bogdan Milićević [a,b], Aleksandar Atanasijević [f], Jelena Živković [b], Andreja Živić [g], Maria Roumpi [c], Themis Exarchos [c,h], Christian Hellmich [d], Stefan Scheiner [d], Hans Van Oosterwyck [e], Djordje Jakovljević [i], Miloš Ivanović [b,f,g], Nenad Filipović [a,b]

[a] Faculty of Engineering, University of Kragujevac, Kragujevac, Serbia
[b] Bioengineering Research and Development Center (BioIRC), Kragujevac, Serbia
[c] University of Ioannina, Ioannina, Greece
[d] Vienna University of Technology, Vienna, Austria
[e] Biomechanics section, Department of Mechanical Engineering, KU Leuven, Belgium
[f] University of Kragujevac Computing Center, Kragujevac, Serbia
[g] Faculty of Science, University of Kragujevac, Kragujevac, Serbia
[h] Ionian University, Corfu, Greece
[i] Coventry University, Coventry, United Kingdom

ARTICLE INFO

Keywords:
Computational platform
Multiscale modeling
User-friendly interface
Open science

ABSTRACT

Background and Objective: : In accordance with the latest aspirations in the field of bioengineering, there is a need to create a web accessible, but powerful cloud computational platform that combines datasets and multiscale models related to bone modeling, cancer, cardiovascular diseases and tissue engineering. The SGABU platform may become a powerful information system for research and education that can integrate data, extract information, and facilitate knowledge exchange with the goal of creating and developing appropriate computing pipelines to provide accurate and comprehensive biological information from the molecular to organ level.

Methods: : The datasets integrated into the platform are obtained from experimental and/or clinical studies and are mainly in tabular or image file format, including metadata. The implementation of multiscale models, is an ambitious effort of the platform to capture phenomena at different length scales, described using partial and ordinary differential equations, which are solved numerically on complex geometries with the use of the finite element method. The majority of the SGABU platform's simulation pipelines are provided as Common Workflow Language (CWL) workflows. Each of them requires creating a CWL implementation on the backend and a user-friendly interface using standard web technologies. Platform is available at https://sgabu-test.unic.kg.ac.rs/login.

Results: : The main dashboard of the SGABU platform is divided into sections for each field of research, each one of which includes a subsection of datasets and multiscale models. The datasets can be presented in a simple form as tabular data, or using technologies such as Plotly.js for 2D plot interactivity, Kitware Paraview Glance for 3D view. Regarding the models, the usage of Docker containerization for packing the individual tools and CWL orchestration for describing inputs with validation forms and outputs with tabular views for output visualization, interactive diagrams, 3D views and animations.

Conclusions: : In practice, the structure of SGABU platform means that any of the integrated workflows can work equally well on any other bioengineering platform. The key advantage of the SGABU platform over similar efforts is its versatility offered with the use of modern, modular, and extensible technology for various levels of architecture.

* Corresponding author.
E-mail address: tijanas@kg.ac.rs (T. Geroski).

https://doi.org/10.1016/j.cmpb.2023.107935
Received 11 May 2023; Received in revised form 6 November 2023; Accepted 18 November 2023
Available online 22 November 2023

1. Introduction

Multiscale modeling is a computational approach that involves modeling a system at length scales, e.g. from the micro to macro scale, to gain a more complete understanding of the system's behavior. This means that prediction of the behavior of the system at a one scale is achieved by incorporating information from other scales using various techniques, such as coarse-graining, upscaling, and hybrid methods. Multiscale modeling is used in a variety of fields, including materials science, biophysics, and drug discovery, to study complex systems that cannot be fully understood using a single scale approach. The main contribution of such combined modeling is that it includes relevant unit processes that are able to effectively capture phenomena that are difficult to observe in vivo or in vitro. Currently, multiscale modeling is mainly implemented using computational approaches, since in the last 20 years various software technologies have been developed to support the integration and coupling of existing single scale models, the managing of the large number of possible simulation runs through automation and the ease of access on high-performance computing (HPC) machines [1]. As part of the Horizon Twinning project "Increasing Serbia's Scientific, Technological, and Innovation Capacity in the Domain of Multiscale Modeling and Medical Informatics in Biomedical Engineering (SGABU)" [2] the main aim is to integrate various solutions and datasets related to cancer, cardiovascular and bone disorders into one multiscale platform. This will enable further validation and parameterization of models, creation of environment for future trends, e.g. in silico clinical trials, virtual surgery, development of prediction models, as well as new opportunities for breakthrough research. Several existing multiscale modeling platforms that can be used to simulate complex systems, include the following:

1. **Virtual Cell**: It is a software framework for modeling and simulating biochemical and biophysical processes across different scales. It supports multiple modeling approaches, including stochastic, deterministic, and hybrid models [3].
2. **OpenMM**: It is a toolkit for molecular simulation that can be used to simulate molecular systems at different scales, ranging from small molecules to large biomolecules [4].
3. **CompuCell3D**: It is a software framework for simulating the behavior of cells and tissues in three dimensions. It includes a variety of models, including reaction-diffusion models, cellular automata, and lattice-based models [5].
4. **SimTK**: It is a platform for the development of multiscale simulations of biological systems. It includes a range of modeling tools, including molecular dynamics, finite element analysis, and systems biology models [6].
5. **CHASTE**: It is a software package for simulating the behavior of cells and tissues in biological systems. It includes a range of modeling tools, including finite element analysis, cellular automata, and ODE-based models [7].

These are just a few examples of the existing multiscale modeling platforms. Of course, there are several other platforms available which cater to a specific domain, for which one can pick the platform that best suits his/her needs. While current multiscale computing software (MCS) has been demonstrated to be beneficial as per its usage, there is a need to further evaluate their added value in the multiscale application development process and identify missing gaps in which new software could provide additional support [1]. Additionally, there are not any platforms that cater to both research and education. To the best of our knowledge, there is not any well-known platform that combines models from multidisciplinary fields in biomedical engineering and medical informatics. Therefore, the main aim of the SGABU platform is to integrate multiscale models and datasets from four different fields: cardiovascular, cancer, tissue engineering, and bone modeling. This is the first proposed integrated platform that will include different areas of bioengineering. This is our greatest contribution and primary objective, as early-stage researchers usually do not have a topic that does not overlap between the fields. Interdisciplinary will be in focus, where the early-stage researchers will have the unique opportunity to experiment with solutions not just from one filed but from several connected fields and be involved in coupled multiscale modeling. In addition, the SGABU platform is designed to be user-friendly and adaptable to the needs of students, researchers, and medical doctors without installing any new software on their local devices because it is executable from any web browser (Mozilla, Chrome, Microsoft Edge). The SGABU platform is designed to be user-friendly and adaptable to primarily suit the needs of students and researchers, or even doctors and other clinical specialists. Although in its early stage, its modular architecture, the versatile code inside the physics solver engine and the well accepted standards to create workflows will allow for the prolonged lifespan and sustainability of the SGABU platform.

2. Materials and methods

The SGABU platform aims to provide a comprehensive collection of models and datasets related to multiscale modeling. The link to the platform is https://sgabu-test.unic.kg.ac.rs/login. No installation is required, and this is the main advantage of the platform, as there are no dependencies of the libraries, software versions, computing resources etc. Indeed, access to all the modules is via the provided link. The integration of multiscale models follows a set of standardized procedures, which allows for secure access to all applications through any internet-connected device and browser. The platform integrates existing computer models in the four aforementioned fields, along with patient-specific databases. Since the platform is envisioned not just to have raw datasets and models, but to be able to carry out simulations with the change of different parameters, visualize the simulation results, interact with the dataset instances, and update the plots, in cases of new datasets/models, frontend and backend should be created by platform administrators. In that case, researchers with new datasets/models should contact platform administrators at sgabu@kg.ac.rs with their request, along with dataset/model description, which can be then integrated on the platform.

The primary objectives of the integration process are to: (1) develop a robust information system that can integrate data, extract information and share knowledge, (2) design and develop appropriate computation pipelines that provide accurate and comprehensive biomedical information from the molecular to the organ level for patients, and (3) integrate advanced mathematical models that can predict the progression of diseases, their relationship with biological markers, and ideally, the tolerance/resistance to different drug families and the existing risks to patients. The integration process can be divided into two main subtasks: (i) integration of datasets (DICOM medical images, tabular data (in csv format) related to biomarkers, TIFF images from experiments, 3D geometries etc.) and (ii) integration of multiscale models (models at the levels of organs, tissue, as well as cellular level).

2.1. Platform architecture

The architecture of the SGABU platform is depicted in Fig. 1 as a hierarchical multilayer schema made up of five layers. At the bottom, lies the **Hardware layer** where virtual instances are deployed. The **Security layer** provides mechanisms for user access management, authentication, authorization, and encrypted communication. The **Workflow layer's** purpose is to give a low-level execution engine to be utilized by the upper layer. The **Back-end layer** provides abstract interfaces, ready to be employed either by the **Front-end**, or other applications built on top of the SGABU platform. Next, we provide details about the concept and implementation of each of these layers.

Hardware layer. In the current state of the SGABU platform, we maintain two distinct deployments: *production* and *staging*. To keep the

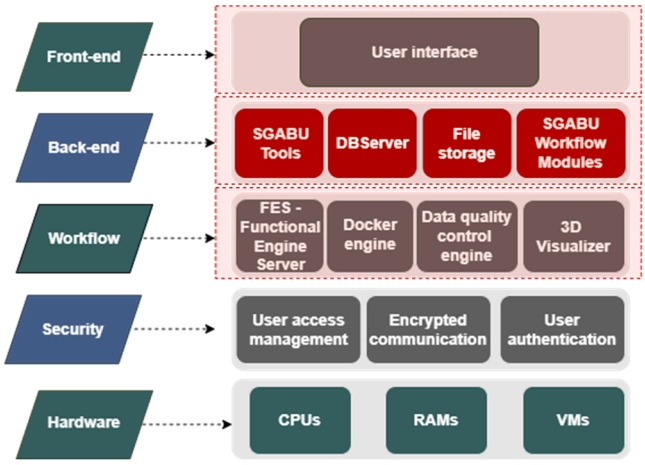

Fig. 1. The architecture of the SGABU platform.

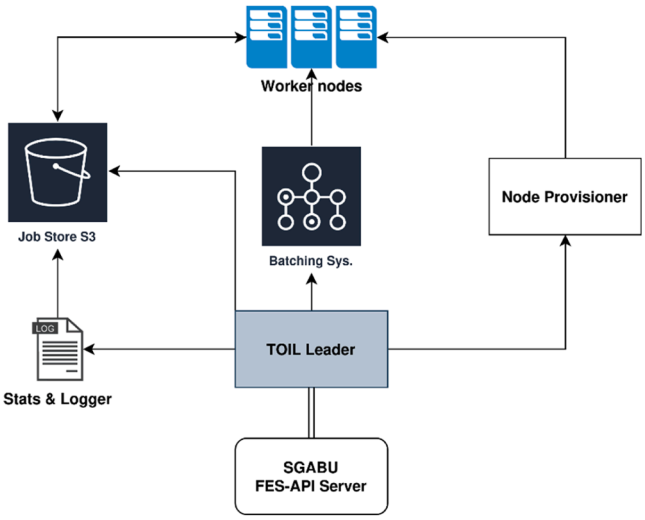

Fig. 2. The execution of the workflow in AWS environment with auto-scaling feature enabled.

SGABU platform agnostic in an infrastructural sense, the *production* resides on virtual instances provided on-premise, while the resources used by *staging* are AWS (Amazon Web Services). AWS provides some interesting possibilities for scaling.

Security layer. All ingress public HTTP traffic is routed by a central NGINX reverse proxy and is SSL encrypted. A separate VPN-secured private network was established for developers and maintainers for accessing the platform's internal infrastructure. In the *production deployment*, we use a separate hardware firewall to protect VM instances that serve SGABU, while in *staging deployment* (AWS) the same functionality is provided by a well-known VPC (Virtual Private Cloud) service. Since the internal network is private, the communication among services can be plain and unencrypted.

Workflow layer. The main purpose of this layer is to act as a middleware between SGABU tools and modules and the underlying infrastructure, thus obscuring the complexity of the infrastructure. The most important objectives of the Workflow layer's design are modularity and reusability, in order to respect the findability, accessibility, interoperability and reusability (FAIR principles) of digital assets. Moreover, the individual tools must be organized, interconnected and orchestrated in a standardized way. In the present day, this implies packaging software using well-known Linux container technologies, such as Docker or Singularity, and orchestrating workflows and pipelines using domain-specific workflow language like WDL (Workflow Description Language) and CWL (Common Workflow Language) [8].

In the SGABU platform, the main workflow executor is the *Functional Engine Server* (FES). This most resource-demanding component is responsible for the execution of the CWL (Common Workflow Language) compatible scientific workflows. FES API is a REST API developed in Python whose primary purpose is to execute, and manipulate various workflows. The lifecycle of such a workflow includes creation, handling inputs and outputs, execution and result acquisition. The significant advantage of FES is an asynchronous execution of workflows as background processes, allowing multiple workflows from different users to run simultaneously. It can be configured to use two different CWL executors: *cwltool* and TOIL [9]. We opted for TOIL in both *production* and *staging* deployments, due to its flexibility.

Especially in the cloud environment, clustering and resource provisioning, features provided by the TOIL workflow manager come to the fore. Thanks to TOIL, FES directly interacts with AWS EC2 API, launching and terminating virtual instances according to the current and provisioned workload, as shown in Fig. 2. Upon workflow creation, in case that the *Leader* acts in the auto-scale mode, the *Node provisioner* launches an appropriate EC2 instance (if necessary), and joins it to the automatically managed Apache Mesos cluster. As soon as an instance joins the cluster, it is ready to execute a workflow requested by FES-API.

The scalability is not only provided when the load is increasing but also when the EC2 instance is not needed anymore. It automatically switches off upon completing the requested workflow and transferring the results to the S3 bucket. This feature significantly contributes to IaaS (Infrastructure as a Service) cost savings.

Another useful open-source utility is a customized Kitware Paraview Glance, which plays the role of the 3D visualizer. It is tightly coupled with FES while performing postprocessing and transformation tasks on 2D/3D simulation data. Thanks to this tight coupling, the user is released from the necessity of transporting large workflow output files for offline analysis.

Back-end layer. SGABU platform's backend follows a model-view-controller design pattern and is built using popular Laravel framework. It provides important built-in features for web applications, including authentication, session management, routing, migration system, etc. To widen SGABU audience, especially among students, we also provided logging with the use of Google account. *DBServer* provides a standard relational database functionality, and *File Storage* gives a user possibility to store large amounts of data for future analysis. *SGABU Workflow Modules* make use of all functionalities and technologies provided by the lower layers.

Front-end layer. SGABU uses Angular framework to build a single-page client experience. The core value proposition of Angular and its ecosystem is to make it possible to build applications that behave sufficiently good on nearly any platform - whether mobile, web, or desktop.

3. Results

The proposed methodology aims to create an e-infrastructure with the capacity to integrate new multiscale models and datasets into a platform that can adapt and evolve to new ideas, and even tackle research challenges. The main dashboard of the SGABU platform (Fig. 3) is divided into sections for each field of research, each one of which includes a subsection of datasets and multiscale models. Upon accessing any of the modules, a help page automatically opens to provide guidelines on how to use a specific model/dataset, along with the theoretical background and resources for additional reading.

3.1. Collection of datasets

Depending on the requirements given by the dataset provider, the datasets can be presented in a simple form as tabular data, or in a slightly smarter manner which requires further tuning using technologies such

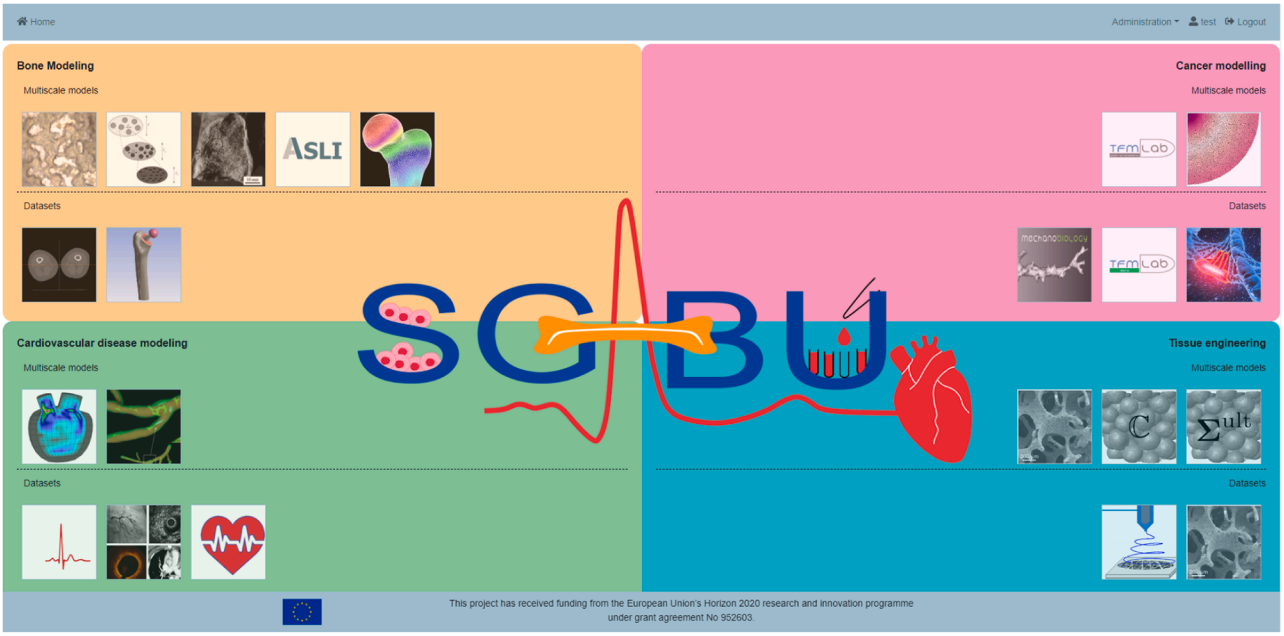

Fig. 3. The main dashboard of the SGABU platform.

as Plotly.js for 2D plot interactivity, Kitware Paraview Glance for 3D view, etc. [10,11]. Plotly.js provides maps, pie charts, bar charts, bubble charts, and gives a wide range of possibilities for user interaction with page elements, which makes it very useful for *what-if* analyses. All provided datasets can be downloaded their original form in a local machine for offline analysis, which is in accordance with the Open Science policy [12]. Up until recently, several datasets have been integrated as part of the platform:

- **Baghdadite** - Baghdadite (Ca3ZrSi2O9) is a specific tissue engineering material. This workflow is integrated as part of the tissue modeling field and shows how respective data produced from nanoindentation studies on baghdadite [13], or data of ultrasound measurements, can be processed to give access to the material stiffness. The respective data can be downloaded through this workflow in form of a CSV-file.
- **Femur geometries** - This workflow is integrated as part of the bone modeling field. This dataset contains the geometries of a human femoral bone with an implant after total hip arthroplasty (THA). Namely, it includes the following geometries - proximal trabecular bone tissue, cortical bone tissue, stem (main body), and femoral head of stem. The geometries of the proximal trabecular and cortical bone tissue are osteotomized based on the surgical protocol of a conventional THA procedure. Furthermore, the cortical bone geometry comprises only the part of the proximal epiphysis and part of the midshaft higher than the isthmus. The aforementioned geometries have been used in a finite element analysis using a third-party commercial software to model the mechanical loading on a human femoral bone with an implant while in single-leg stance [14].
- **Stenosis cases** - This workflow is integrated as part of the tissue cardiovascular modeling field. The dataset contains three arterial cases with different percentage of diameter stenosis (DS), one with 2 % DS, one with 79 % DS and one bifurcated segment with 80 % DS. There are also other metrics which are presented on this field of the platform for each case. These metrics include the total vessel length, the lesion vessel length which represents the stenosis area in the artery, the reference vessel diameter (RVD) and the minimum lumen diameter (MLD) of the vessel [15].
- **Oral cancer** - This workflow is integrated as part of the cancer cardiovascular modeling field. The dataset for Oral cancer contains four CSV-files that provide information about the blood and tissue genes of each patient, the different timepoints for the genes of each patient and information obtained from imaging. All these files can be easily downloaded by clicking on the appropriate button located on the right side of the screen [16].
- **Mechanobiology** – This workflow is integrated as part of the cancer modeling field. The user will see a panel with two tabs (labelled as "Relaxed" and "Stressed") and four images in each tab. These data correspond to a classical traction force microscopy (TFM) experiment [17]. In this experiment, cells cultured in vitro within a Polyethylene glycol (PEG) hydrogel that contains fluorescent beads are imaged by means of confocal microscopy before and after the addition of mechanical inhibition. Since cells need to exert forces to migrate, they deform the surrounding hydrogel causing movements on the beads. TFM quantifies the movements of these beads and through constitutive equations recovers the cell forces [18]. In the SGABU platform, we provide a dataset that would allow for the computation of 3D cell forces around a growing angiogenic sprout.
- **TFMLAB data** – This workflow is integrated as part of the cancer modeling field. The data correspond to raw and processed data from a 3D traction force microscopy (TFM) experiment (see previous point, [18]). In SGABU, we provide a dataset showing all the intermediate steps that are needed to get to a measurement of the force-induced matrix displacements.
- **LVAD** – This workflow is integrated as part of the cardiovascular modeling field. LVAD (Left Ventricular Assist Device) is a type of mechanical pump that supports the normal function of the left ventricle of the heart in order to maintain normal cardiac output and sustain oxygen supply to the rest of the body. The importance of LVAD for patients with advanced heart failure has been extensively studied on whether patients using LVAD with concomitant treatment with drugs can achieve the level of cardiac recovery similar to a healthy individual. The dataset contains the clinical characteristics of a studied population (155 in total), which includes three groups of patients, namely the (i) the heart transplant candidates, (ii) LVAD implanted and (iii) LVAD explanted patients, as well as healthy subjects which is the control group. In addition, the dataset contains data of cardiac and respiratory measurements at rest and in response to maximal anaerobic exercise for the four different groups [19].

- **Hip joint** – This workflow is integrated as part of the bone modeling field. This dataset contains 301 DICOM images, obtained from a CT scanner [20]. The scans include one hip joint with artificial femoral prosthesis and one healthy hip joint. A user can move through the dataset by clicking on left or right arrows next to the image, or by using the slider function below the image.
- **Electrospinning** - This workflow is integrated as part of the tissue modeling field. Electrospinning is a technique for creating fibers, and it includes electrohydrodynamic process and high voltage electricity [21]. During electrohydrodynamic process, a jet is created by using liquid solution. The deposition of solid fiber on the collector is product of stretching the charged jet. It was necessary to make gelatin scaffolds with micro/nano scale, which are used to regenerate wound tissue. For good stimulation of tissue regeneration, it is necessary of projecting biomaterials with optimal characteristics, which can be determined using relations between their material properties. The dataset includes data in tabular format that relate optimal values for the material properties of the liquid solution with other parameters, e.g., like the applied voltage. The values of the different parameters in the table can be sorted and downloaded on a local machine.

3.2. Detailed use case example of a dataset

The Left Ventricular Assist Device (LVAD) dataset belongs to the Cardiovascular disease modeling module and can be accessed via the main dashboard of the platform. LVAD is a mechanical pump that supports the normal function of the heart's left ventricle. This pump cannot fully replace the heart, but it supports its action by maintaining normal cardiac output and oxygen supply to the rest of the body. The importance of LVAD for a patient whose life is threatened from heart malfunctioning has been extensively studied on whether patients with implanted LVAD and concomitant treatment with drugs can achieve heart restoration equivalent to that of healthy individuals after the removal of the LVAD. Fig. 4 shows a table which includes the clinical characteristics of a studied population divided into four groups [19]. From the table it is shown that the studied population consists of 155 male subjects in total, where the number of heart transplant candidates (HTx) is 24, the number of patients with implanted LVAD is 18, the number of patients who had an LVAD implanted and after rehabilitation being explanted is 16, while the rest 97 constitute healthy individuals. The table of clinical characteristics includes generic measures like age, height, body weight, etc. and the drugs given to patients for medication treatment.

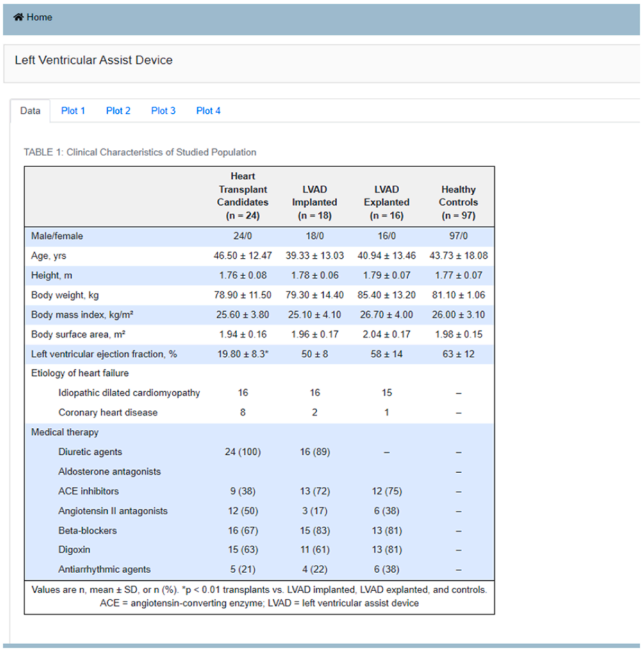
Home

Left Ventricular Assist Device

Data | Plot 1 | Plot 2 | Plot 3 | Plot 4

TABLE 1: Clinical Characteristics of Studied Population

	Heart Transplant Candidates (n = 24)	LVAD Implanted (n = 18)	LVAD Explanted (n = 16)	Healthy Controls (n = 97)
Male/female	24/0	18/0	16/0	97/0
Age, yrs	46.50 ± 12.47	39.33 ± 13.03	40.94 ± 13.46	43.73 ± 18.08
Height, m	1.76 ± 0.08	1.78 ± 0.06	1.79 ± 0.07	1.77 ± 0.07
Body weight, kg	78.90 ± 11.50	79.30 ± 14.40	85.40 ± 13.20	81.10 ± 1.06
Body mass index, kg/m²	25.60 ± 3.80	25.10 ± 4.10	26.70 ± 4.00	26.00 ± 3.10
Body surface area, m²	1.94 ± 0.16	1.96 ± 0.17	2.04 ± 0.17	1.98 ± 0.15
Left ventricular ejection fraction, %	19.80 ± 8.3*	50 ± 8	58 ± 14	63 ± 12
Etiology of heart failure				
Idiopathic dilated cardiomyopathy	16	16	15	–
Coronary heart disease	8	2	1	–
Medical therapy				
Diuretic agents	24 (100)	16 (89)	–	–
Aldosterone antagonists				–
ACE inhibitors	9 (38)	13 (72)	12 (75)	–
Angiotensin II antagonists	12 (50)	3 (17)	6 (38)	–
Beta-blockers	16 (67)	15 (83)	13 (81)	–
Digoxin	15 (63)	11 (61)	13 (81)	–
Antiarrhythmic agents	5 (21)	4 (22)	6 (38)	–

Values are n, mean ± SD, or n (%). *p < 0.01 transplants vs. LVAD implanted, LVAD explanted, and controls.
ACE = angiotensin-converting enzyme; LVAD = left ventricular assist device

Fig. 4. Clinical Characteristics of Studied Population.

The aim of this study was to compare cardiac and respiratory measurements at rest and maximal graded cardiopulmonary exercise for the four different groups. Only subjects were included who chose to provide a consent form and had the ability to perform treadmill exercise tests and exercise beyond anaerobic threshold. For credible results, cardiac and respiratory measurements were acquired, using a valid and reproducible method, namely the inert gas rebreathing method, at rest and maximum effort. The group of the LVAD explanted patients and healthy controls performed the Bruce protocol, while the group of the heart transplant candidates and the LVAD implanted patients performed the modified Bruce protocol [19]. Measures of arterial blood pressure using cuff sphygmomanometry and estimation of cardiac output using the Innocor device were acquired. The cardiac power output was calculated by using the following formula:

$$CPO = (QTxMAP)xK,$$

where CPO is the cardiac power output measured in watts, QT is the cardiac output in liters per min, MAP is the mean arterial pressure in millimeters of mercury and K is an appropriate conversion factor. The mean arterial pressure (MAP) was calculated by the following formula:

$$SBP + 0.412x(SBP - DBP),$$

where SBP is the systolic blood pressure and DBP is the diastolic blood pressure. Systemic vascular resistance to blood flow was defined as the ratio between the mean arterial pressure and cardiac output, multiplied by an appropriate factor for unit conversion. The values of the above parameters along with a few more are summarized in the table of Fig. 5.

Based on the tabular data of Fig. 5, a statistical analysis was performed using a third-party commercial software, and differences in measured variables among the different groups were tested with a one-way analysis of variance. Moreover, a post hoc Tukey test was performed to identify groups that differed significantly from one another. A more detailed description can be found in [19]. The graphs produced from the statistical analysis are hosted inside the LVAD dataset and are accessible in different sections (Plot 1, Plot 2, Plot 3 and Plot 4) which can be accessed from the top left of the page (Fig. 6).

Plot 1, which is the graphical chart in Fig. 6, shows the peak exercise power cardiac output (*y-axis*) for the four different subject groups with respect to their age (*x-axis*). In the graphical chart, most of the orange rectangular points which correspond to heart transplant candidates (HTx), are positioned below a dashed line which represents the threshold value for heart transplantation referral. In addition, the LVAD implanted (green triangles) and explanted subjects (red circles) present a higher peak power cardiac output than the untreated heart transplant candidates. Lastly, from the graphical chart it is also evident that some LVAD explanted subjects (red circles) achieved a level of peak exercise power cardiac output similar to that of healthy controls (blue diamonds).

Plot 2, which is the graphical chart depicted in Fig. 7, shows the peak oxygen consumption (*y-axis*) for each subject in the four different groups with respect to their age (*x-axis*). Similarly, most of the heart transplant candidates (orange rectangles) are located below the dashed line which represents the cutoff value for heart transplantation referral. LVAD implanted (green triangles) and LVAD explanted subjects show an improved peak oxygen consumption than the untreated heart transplant candidates (orange rectangles). Lastly, note also that the majority of the LVAD explanted subjects (red circles) achieved equivalent values of peak oxygen consumption with that of healthy individuals.

Plot 3 includes the graph depicted in Fig. 8, which shows the ratio of the peak cardiac power output to peak oxygen consumption (*y-axis*) with

TABLE 2: Resting and Peak Exercise Cardiac and Physical Function Variables in HTx, Implanted and Explanted LVAD Patients, and Healthy Controls

	Heart Transplant Candidates (n = 24)	LVAD Implanted (n = 18)	LVAD Explanted (n = 16)	Healthy Controls (n = 97)
Sitting rest				
Heart rate, beats/min	76.7 ± 19.7	72.6 ± 13.3	73.3 ± 6.2	65.7 ± 10.6
Stroke volume, ml	49.1 ± 12.3*	76.7 ± 17.0	71.1 ± 11.3	73.7 ± 18.0
Systolic BP, mm Hg	94.5 ± 17.5	95.3 ± 21.1	105.2 ± 15.8	123.3 ± 11.7
Diastolic BP, mm Hg	61.4 ± 10.3	63.3 ± 17.9	70.9 ± 12.7	76.3 ± 9.1
Mean arterial BP, mm Hg	74.4 ± 12.1	72.8 ± 15.6	85.5 ± 12.6	95.7 ± 8.98
Cardiac output, l/min	3.53 ± 0.66*	5.5 ± 1.4	5.2 ± 0.8	4.87 ± 1.20
Cardiac power output, W	0.59 ± 0.16*	0.89 ± 0.23	0.94 ± 0.20	1.02 ± 0.22
Vascular resistance, dyn/s/cm	1.735 ± 357*	1.143 ± 433	1.351 ± 293	14.85 ± 509
Oxygen consumption, ml/min	314.4 ± 54.2	371 ± 47	407 ± 35	374 ± 43
Oxygen consumption, ml/kg/min	4.32 ± 0.92	4.74 ± 0.56	4.88 ± 0.09	3.63 ± 0.66
Peak exercise				
Heart rate, beats/min	101.9 ± 21.6*	142.3 ± 26.0§	162.8 ± 12.9	173.9 ± 16.7
Stroke volume, ml	82.9 ± 22.2	88.9 ± 16.8	90.6 ± 15.2ı	116.9 ± 18.5
Systolic BP, mm Hg	94.9 ± 16.3*	115.6 ± 25.0§	140.1 ± 21.9ı	199.1 ± 18.4
Diastolic BP, mm Hg	59.4 ± 10.1	72.0 ± 14.5	78.1 ± 12.6ı	66.0 ± 14.3
Mean arterial BP, mm Hg	74.0 ± 11.8*	86.9 ± 17.9§	103.5 ± 18.2ı	120.8 ± 11.0
Cardiac output, l/min	8.12 ± 1.52*	12.4 ± 1.9§	14.7 ± 2.37ı	20.3 ± 3.9
Cardiac power output, W	1.31 ± 0.31*	2.37 ± 0.67§	3.45 ± 0.72ı	5.36 ± 0.94
Vascular resistance, dyn/s/cm	758 ± 195	569 ± 118	583 ± 159ı	495 ± 116
Oxygen consumption, ml/min	916 ± 227*	1.814 ± 422§	2.511 ± 420ı	3.090 ± 740
Oxygen consumption, ml/kg/min	12.0 ± 2.2*	20.5 ± 4.3§	29.8 ± 5.9ı	36.4 ± 10.3
Arterial-venous oxygen difference, ml O2/100 ml of blood	11.3 ± 2.2*	15.1 ± 4.1§	17.2 ± 2.3	18.2 ± 3.7
Respiratory exchange ratio	1.10 ± 0.15	1.13 ± 0.07	1.11 ± 0.07	1.11 ± 0.08

Values are mean ±SD. *p < 0.05 transplants vs. LVAD implanted, LVAD explanted, and controls. †p < 0.05 controls vs. transplants, LVAD explanted, LVAD implanted. ‡p < 0.05 controls vs. transplants and LVAD implanted. §p < 0.05 LVAD implanted vs. LVAD explanted, and controls. ıp < 0.05 LVAD explanted vs. controls.
BP = blood pressure; HTx = heart transplant candidate; LVAD = left ventricular assist device.

Fig. 5. Resting and Peak Exercise Cardiac and Physical Function Variables in HTx, Implanted and Explanted LVAD Patients, and Healthy Controls.

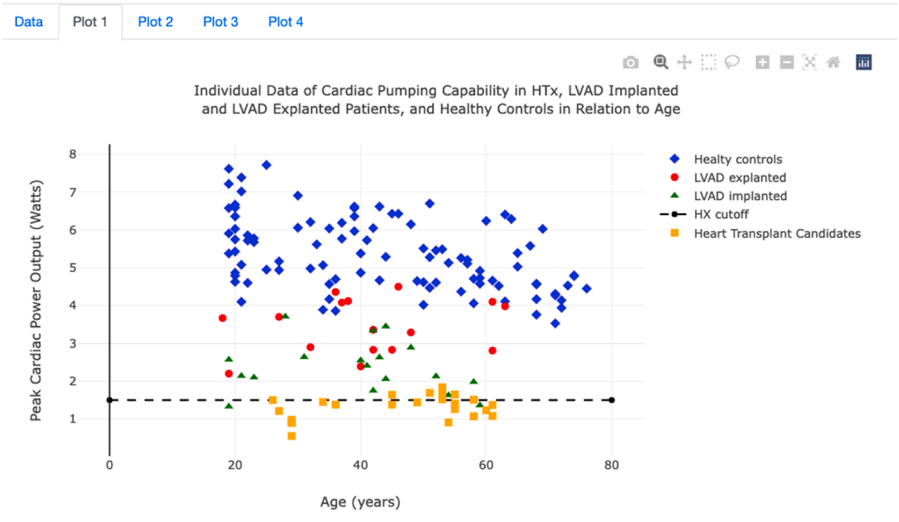

Peak exercise cardiac power output in healthy controls (blue diamonds), LVAD explanted (orange circles), LVAD implanted (gray triangles), and heart transplant candidates (red squares) individual data in relation to age. Six of 16 (38%) LVAD explanted patients achieved a level of peak exercise cardiac power output equivalent to that of healthy controls. Dashed line (HTx cutoff) represents clinical threshold value for heart transplantation referral.

Fig. 6. Individual Data of Cardiac Pumping Capability in HTx, LVAD Implanted and LVAD Explanted Patients, and Healthy Controls.

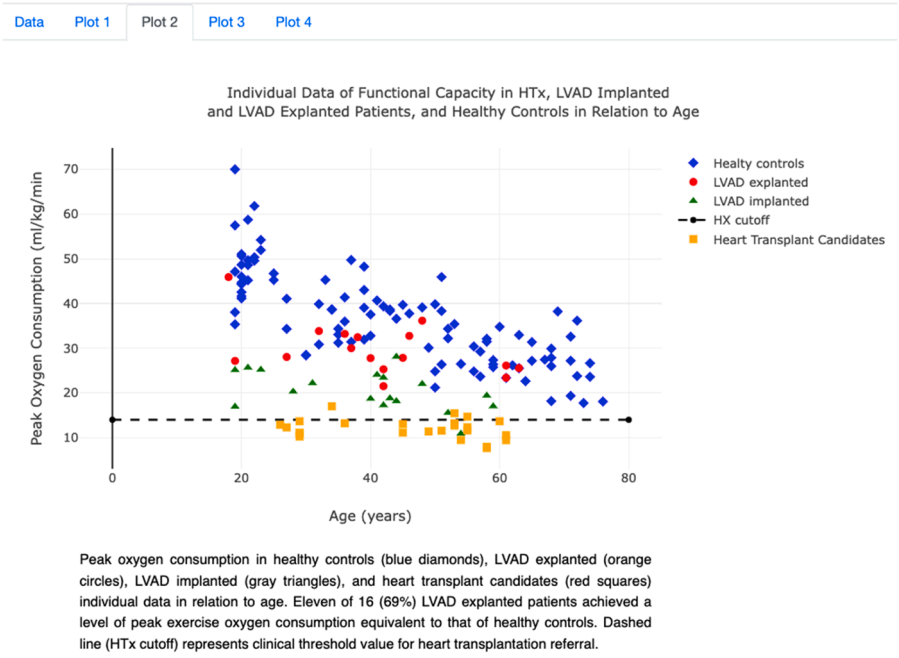

Fig. 7. Individual Data of Functional Capacity in HTx, LVAD Implanted and LVAD Explanted Patients, and Healthy Controls in Relation to Age.

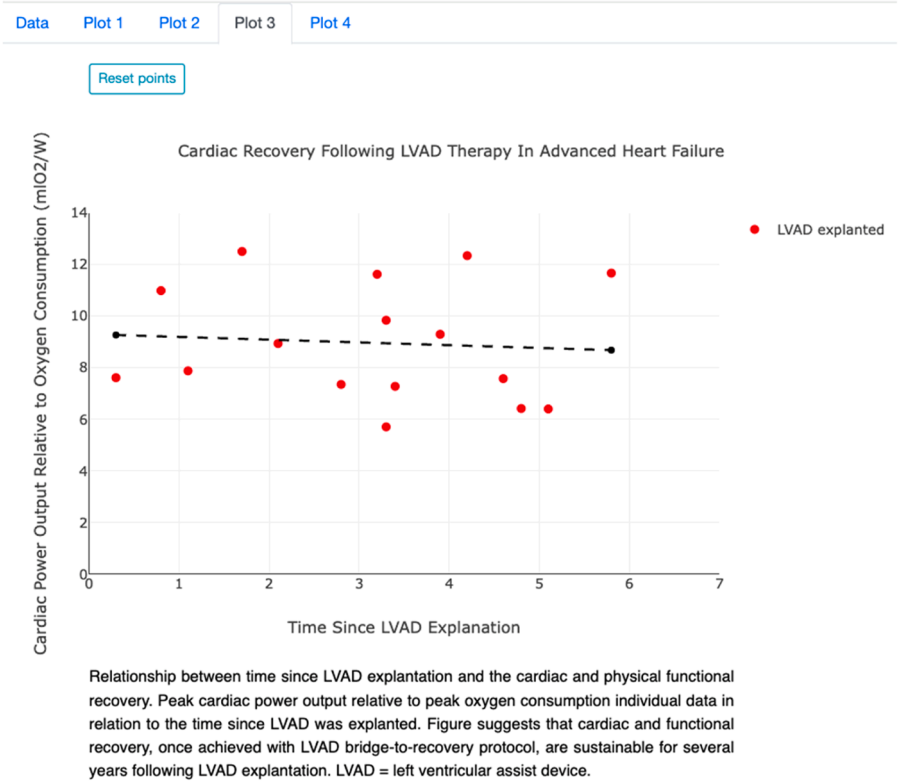

Fig. 8. Cardiac Recovery Following LVAD Therapy in Advanced Heart Failure.

respect to the time since the LVAD removal (*x-axis*) for the 16 LVAD explanted subjects. The trend of the dashed line in the graph, which represents the regression line, suggests that cardiac and functional recovery, once achieved with medication treatment and the implantation of LVAD, is sustained for several years after the removal of LVAD. Note also that the platform allows the user to interact with the graph in a way where he/she can click on individuals points on the graph and remove those points from the calculation of regression analysis. In that way, the slope of the regression line changes accordingly. The excluded points can be reset from the "Reset points" option located above the graph.

Finally, Plot 4 includes a bar graph (Fig. 9), which graphs the peak exercise cardiac power output (red bars) and oxygen consumption (blue bars) in each one of the four different groups as a percentage with respect to the control group of healthy subjects. Thus, the red and blue

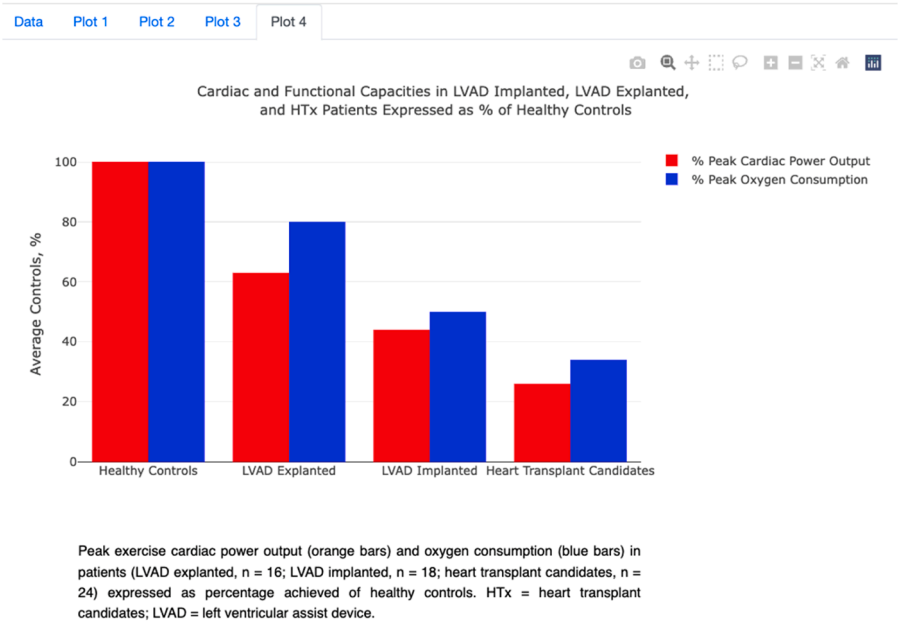

Fig. 9. Cardiac and Functional Capacities in LVAD Implanted, LVAD Explanted, and HTx Patients Expressed as% of Healthy Controls.

bars of the group with the healthy subjects present values of 100 %, since this group is the control group, while the rest of the groups present a decreased trend from the LVAD explanted group to the HTx group. In that trend, the peak exercise power cardiac output (red bars) shows a more distinct decline than the peak oxygen consumption (blue bars). Lastly, note that the platform allows user interaction of the bar graph by enabling or disabling each variable upon clicking its name on the right side of the graph.

3.3. Collection of multiscale models

Most of the SGABU multiscale models are built as Common Workflow Language (CWL) workflows. The usage of Docker containerization for packing the individual tools and CWL orchestration for describing inputs, outputs and intermediate outcomes, results in intrinsic findability, accessibility, interoperability, and reusability (FAIR principles). In practice, this means that any of these workflows can work equally well on any other bioengineering platform. The effort involved in offering CWL-type workflows in SGABU is divided into two main actions: firstly create a CWL implementation on the FES (Functional Engine Service) and develop the user interface, and secondly create UI elements as input forms with validation of numeric values, file types, etc., as well as tabular views for output visualization, interactive diagrams, 3D views and animations. Up until recently, several models have been integrated as part of the SGABU platform:

- **BonePoreDense** – This model is integrated as part of the bone modeling field. The model is based on the model published in [22]. Users are expected to fill out the following forms: Workflow name, Different lacunar porosities, Resolution of contourplots. Except for the "Workflow name", all input forms are numerical and value ranges are provided for the users. The workflow name can be freely chosen. For the "Different lacunar porosities" a value between 1 and 100 should be entered. The value of this variable is the volume fraction Φ_{lac}, as percentage, of the lacunar pores contained in a macroscopic unit cell of bone. The "Resolution of contourplots" stands for the number of considered values for the vascular porosity and extracellular mass density each. A value between 10 and 100 should be entered.
- **BoneMinOrg** – This model is integrated as part of the bone modeling field. The model is based on the model published in [22]. Users are expected to fill out the following forms: Workflow name, Lacunar porosity in [%], Different vascular porosities, Resolution of contourplots. Except for the "Workflow name", all input forms are numerical and value ranges are provided for the users. The workflow name can be freely chosen. For the "Lacunar porosity in [%]" a value between 0 and 10 should be entered. The value of this variable is the volume fraction Φ_{lac}, as percentage, of the lacunar pores contained in a macroscopic unit cell of bone. The "Different vascular porosities" refers to the volume fraction Φ_{vas}, as percentage, of the vascular porosity in a macroscopic unit cell of bone. For this parameter input values range from 1 to 100. Lastly, the "Resolution of contourplots" stands for the number of considered values for the apparent organic mass density and the apparent mineral mass density each. A value between 10 and 100 should be entered.
- **ASLI** – This model is integrated as part of the bone modeling field. ASLI is a tool that gives users the ability to provide functionally graded lattice infills to 3D geometries. The provided infill is constructed out of unit cells, described by implicit functions, whose type, size and feature can be varied locally based on user provided inputs. The resulting geometries can be 3D printed, or used to create FE-models for computational analysis [23].
- **Corrosion pit** – This model is integrated as part of the bone modeling field. The model of corrosion has been developed based on Cellular Automata (CA) theory. Evolution of each CA cell occurs through a series of synchronous updates of all cells, governed by a set of rules. The computational modeling of multi-pit corrosion in medical implants based on cellular automata is divided into two submodels - pit initiation and growth models. The state of each cell is represented by a predefined interval in the range of 0 – 255, where an uncorroded cell has the value of 0 and a totally corroded cell the value of 255. This means that we look at the surface as an image and prescribe certain rules, which define where the corrosion pit will appear (corrosion pit initiation) and then later how it will develop (corrosion growth model) [24].
- **Parametric Heart** – This model is integrated as part of the cardiovascular modeling field. A parametric heart model of the left ventricle is used to simulate the cardiac cycle with patient-specific dimensions, which are given as inputs by the user. Based on user-

provided values for the different parameters, the geometry of the left ventricle is generated and a finite element simulation is run with prescribed boundary conditions [25]. Boundary conditions consist of inlet and outlet velocities and/or pressures, which are prescribed to the valves of the heart. Users are also allowed to change the stiffness of the left ventricle wall, and the calcium concentration which controls the muscle contraction.

3.4. Detailed use case example of a model

The access to the Finite Element Analysis (FEA) of Femoral Bone, which belongs to the Bone Modeling module on the SGABU platform, is provided through the main dashboard. The aim of this model is to show the effect that different bodyweight and material properties can have on the stress and displacement fields of a human femoral bone when in single-leg stance. The geometry of the femoral bone used for the FEA comprises the cortical and trabecular bone tissue in the proximal epiphysis, and is presented in Fig. 10. To develop digitally volumetric geometries of both tissues, a semi-manual segmentation method from computed tomography (CT) images was employed. For the presented model herein, each body (trabecular and cortical bone) is assumed to behave as a homogeneous, isotropic, linear elastic material, and thus only two elastic constants are needed to fully describe their constitutive equations. For this model, the Young's modulus and Poisson's ratio were considered to describe the mechanical response of each body, whose default values have been adopted from the literature ([26,27,28]). Users are able to change these values as long as the new values are within the allowable range indicated below of each input box. Fig. 11 shows a preview of the four boxes that take as input appropriate numeric values for the material properties of each body, and two additional boxes namely the "Workflow name" which takes as alphanumeric input the name of a particular workflow and "Body weight force" whose numeric input value describes the effect of a different bodyweight.

Regarding the boundary conditions (Fig. 12), the distal end of the model is kept fixed and seven additional forces are applied proximally, in particular three at the femoral head, three at the lateral side of the great trochanter and the last one below the great trochanter. The values for the applied forces have been adopted from the literature [29]. The F_1force, whose value can be changed by the user, corresponds to the force transferred from the hip due to body weight to the femur. The numeric value of that force has been chosen to be controlled by the user, due to the fact that it has the highest value and its change will have the most profound effect on the simulation results. The force due to body weight is calculated using the following equation:

$$BWF = mxg,$$

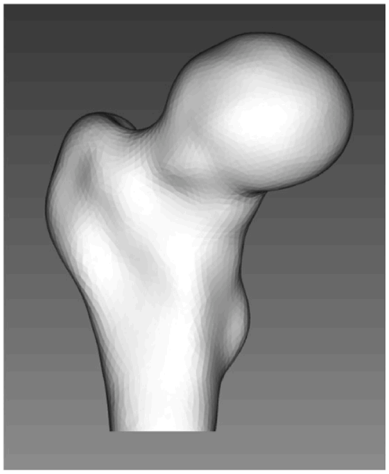

Fig. 10. Femoral bone geometry.

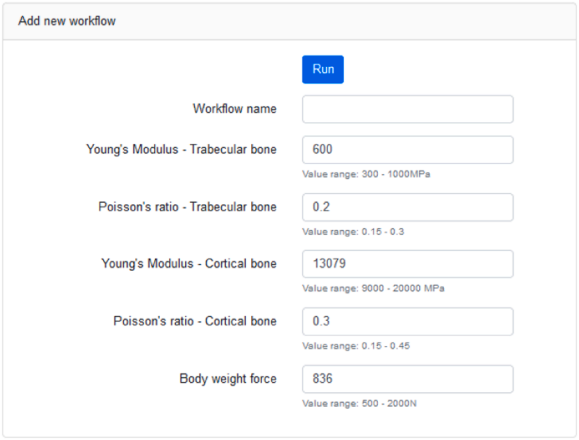

Fig. 11. Defined material properties and body weight force.

where *BWF* stands for the body weight force measured in Newtons, m is the body mass in kg, and g is the acceleration of gravity (approximately 9.81 m/s^2).

Upon entering appropriate input values for the model, users are able to run a simulation of the static linear analysis which models the loading of the femur when in single-leg stance. The solver used to solve the equations that describe the model is integrated inside the in-house PAK software, which has been developed and tested over decades at the University of Kragujevac.

After the successful completion of a simulation run, users are able to visualize in a color-coded fashion the displacement (Fig. 13a) and stress (Fig. 13b) profiles at the femoral bone. Values closer to red correspond to maximum values and values closer to blue correspond to minimum values. The results presented in these two figures correspond to a simulation run with default input values for material properties and body weight. With the simulation results, user can get better understanding of areas at the femoral bone which present the highest stress values and are candidate areas for initiation of cracks and bone fracture.

4. Discussion

There are several platforms available which cater to a specific biomedical domain, for which one can pick the platform that best suits his/her needs. However, there are not any platforms that combine models from multidisciplinary fields in biomedical engineering and medical informatics. SGABU platform is the first that deals with this challenge. Tu further evaluate the SGABU platform, it was tested among 21 users whom had been given access to the platform and afterwards were required to fill a questionnaire that would reflect their impressions of the SGABU platform. These potential users participated in the demonstration of the SGABU workshop named "SGABU platform" on 08/12/2022. At the beginning of the survey some personal information was requested for statistical reasons, although all the collected data were anonymized such that it would not be possible to identify afterwards each survey participant on the basis of his/her given responses. From the collected personal information, it was shown that the majority of the participants were at age up to 30 years old as they were mostly students of Masters and PhD level. The age distribution of the SGABU platform test users is shown in Fig. 14. Out of the 20 participants, 11 were PhD students and 9 were MSc students. The nationalities of the participants were as following: 8 from Greece, 6 from Serbia, and one per countries India, Pakistan, Germany, Italy, Croatia, Bosnia and Herzegovina.

The nationalities of the participants were as following: 8 from Greece, 6 from Serbia, and one per countries India, Pakistan, Germany, Italy, Croatia, Bosnia and Herzegovina. Out of the total number of participants, 13 were male and 7 were female (Fig. 15).

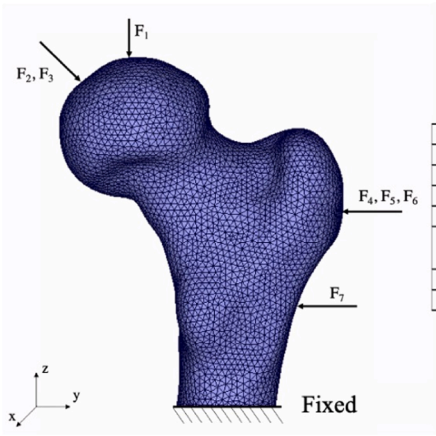

Position	Force	F_x [N]	F_y [N]	F_z [N]
F_1	Body weight	-	-	-836.0
F_2	Hip contact	32.8	54	-229.2
F_3	Intersegmental resultant	12.8	8.1	-78.2
F_4	Abductor	-4.3	-58	86.5
F_5	Tensor fascia latae, proximal part	-11.6	-7.2	13.2
F_6	Tensor fascia latae, distal part	0.7	0.5	-19
F_7	Vastus lateralis	-18.5	0.9	-92.9

Fig. 12. Boundary conditions.

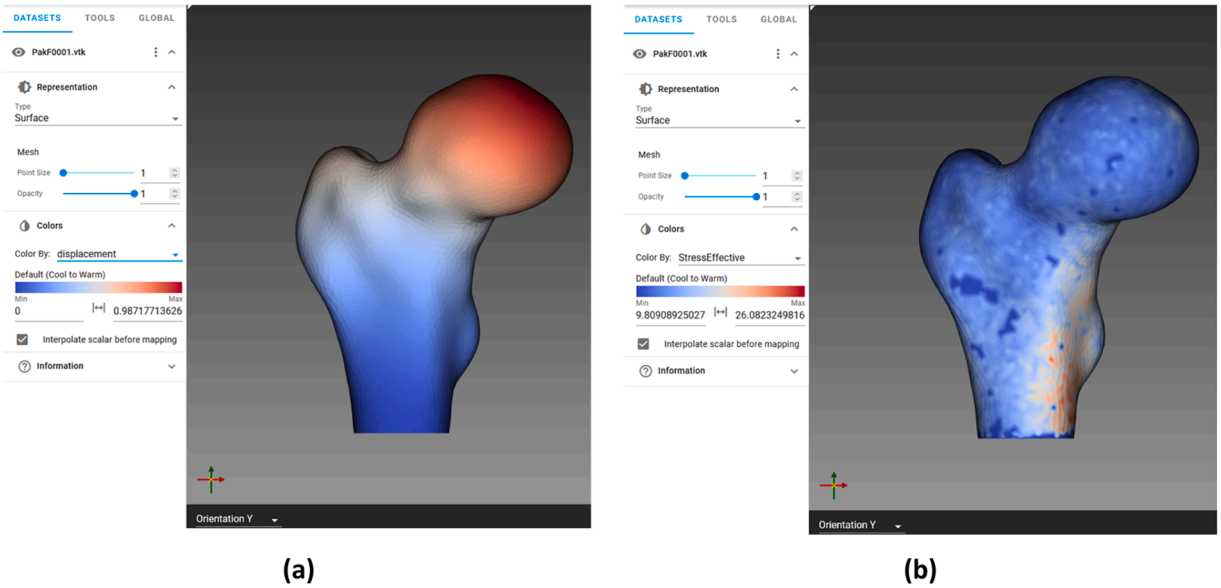

Fig. 13. Model results for (a) total displacement profile; and (b) equivalent Von Mises stress at the femoral bone.

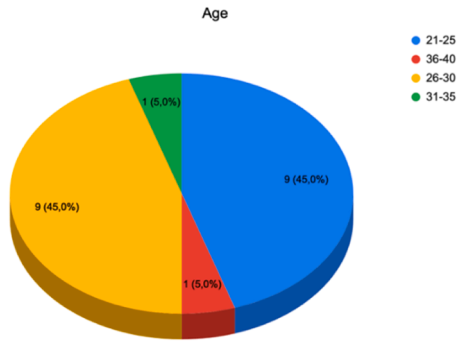

Fig. 14. Age distribution of the SGABU platform test users.

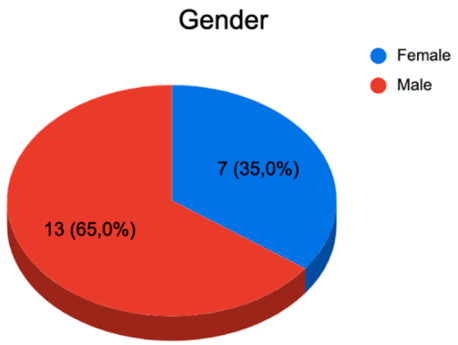

Fig. 15. Gender distribution of the SGABU platform test users.

The users were then required to test the platform and its individual modules and respond to several questions. The main points in the survey were related to the efficiency, performance, complexity and usability of the presented platform and its tools. First request was related to check whether the existing modules were of interest to the users based on their education and research interests. This was reflected through the question "Which of demonstrated SGABU fields would you use in your daily practice?". The responses are given in Fig. 16. It can be seen that Cardiovascular module is of highest interest, yet all modules have captured the attention of the participants.

For requests related to their impressions of the overall platform, the users were required to respond in what degree they agree with several statements. This was reflected through the question "For each of the following statements, mark one box that best describes your impressions

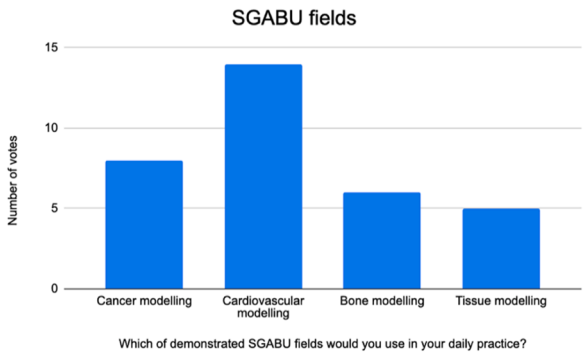

Fig. 16. Response to SGABU target fields.

on the SGABU platform" (Fig. 17Fig. 17. Response to SGABU platform impressions.). It can be seen that the majority of students liked the platform overall, although several participants were unsure whether they would use it in their everyday research. This may derive from the fact that some participants were not from any overlapping area of research with biomedical engineering and medical informatics and did not fully comprehend in a short time the platform and its modules.

For requests related to their impressions of individual modules, the users were required to respond in what degree they agree with several statements. This was reflected through the question "For each of the following statements, mark one box that best describes your impressions on the SGABU modules" (Fig. 18). Similarly, to the previous question, the vast majority of the students gave a positive review for the integrated models and datasets, however for a few participants some individual modules were hard to understand.

From the data obtained through the questionnaire, the generated information has guided the continuous development of the SGABU platform. Their responses provide great feedback for the improvement of the platform and its individual modules. Although the platform is dedicated primarily to students of various levels of education, it has shown great potential to become a useful tool not just in education, but also in research and knowledge sharing. However, it should be stated that from a technical point of view there are some limitations of the platform. Currently, the total upload capacity is 500 MB and the machine is equipped with 24 cores to execute different workflows, which implies that the platform can accept up to 24 users who can concurrently run simulations using 1 core each. This comes from the deployment machine where our workflows were executed. The capacities can be increased automatically if deployed on AWS, as described above, when auto-scaling feature of TOIL workflow manager enables running each workflow as a separate short-running EC2 instance, providing as much resources as required. Another limitation of the models integrated on the platform is that some simulations are executed serially in its core, so waiting time to finish the simulation may be prolonged. This means that future work will be directed towards the parallelization of the simulations, so that the running time is reduced.

5. Conclusions

This paper describes the SGABU platform, developed to integrate multiscale models and datasets in the fields of cardiovascular, bone, tissue and cancer modeling. The key advantage is the utilization of new, contemporary and distinct technology for its many levels of architecture. Because these technologies are completely independent of the underlying infrastructure, the platform may be simply transferred to any private or public cloud as necessary. Students and scholars who use the platform get several benefits. For example, users can use the SGABU platform without installing any new software on their local devices because it is executable from any web browser (Mozilla, Chrome, Microsoft Edge). Platforms like SGABU are more than just common software products with a defined purpose and a short to medium lifespan. Throughout the conception and development of the SGABU platform, two critical elements have been addressed: (i) all of the components were created using industry-standard frameworks and interfaces, and (ii) FAIR principles were closely followed due to the use of well-known workflow management systems. Still in its development stage, the platform has been pilot tested among 21 users who expressed their satisfaction with individual modules as well as the overall platform. From their responses, it was evident that there is an interest for such an integrated platform, which covers topics on several fields in biomedical engineering and medical informatics, and offers a friendly user interface. The end result is a solution that is portable, extendable, and for the time being, ready to serve students and researchers. In the future, upon further upgrading the features of the platform, we aim for its integration into the clinical practice.

Statements of ethical approval

Not applicable

Funding

This research is also supported by the project that has received funding from the European Union's Horizon 2020 research and innovation programmes under grant agreement No 952603 (SGABU project). This article reflects only the author's view. The Commission is not responsible for any use that may be made of the information it contains. T.G., A.V., B.M. and N.F. also acknowledge the funding by the Ministry of Science, Technological Development and Innovation of the Republic of Serbia, contract number [451-03-47/2023-01/200107 (Faculty of Engineering, University of Kragujevac)].

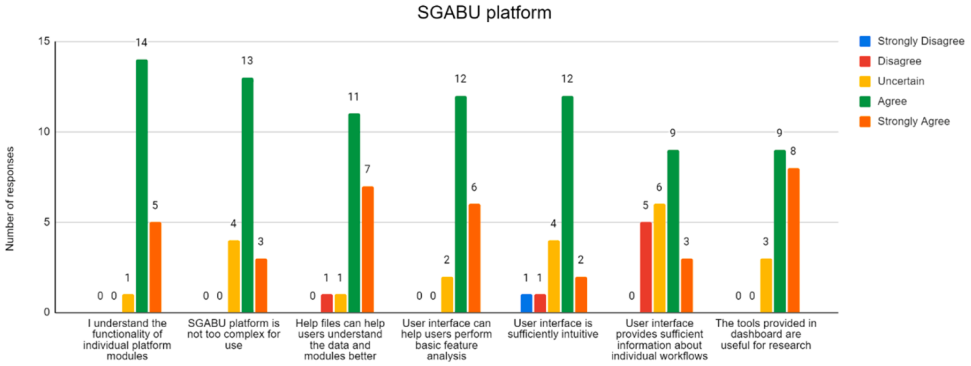

Fig. 17. Response to SGABU platform impressions.

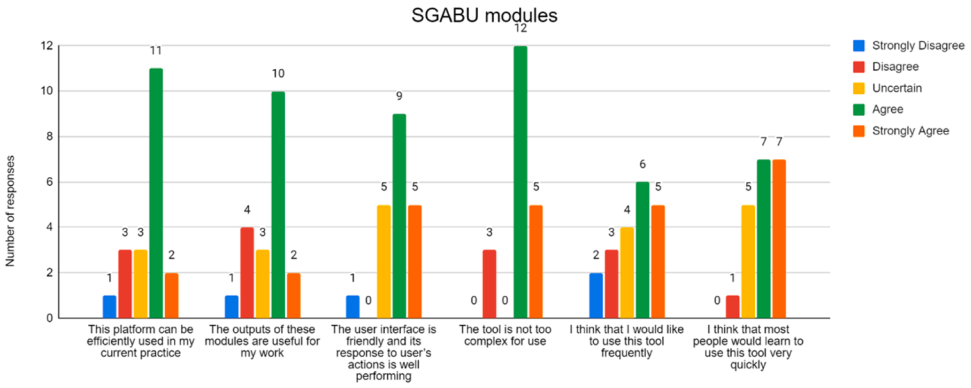

Fig. 18. Response to SGABU individual modules impressions.

Declaration of Competing Interest

The authors declare that they have no known competing financial interests or personal relationships that could have appeared to influence the work reported in this paper.

References

[1] D. Groen, J. Knap, P. Neumann, D. Suleimenova, L. Veen, K. Leiter, Mastering the scales: a survey on the benefits of multiscale computing software, Philos. Trans. R. Soc. A 377 (2142) (2019), 20180147.

[2] "Increasing scientific, technological and innovation capacity of Serbia as a Widening country in the domain of multiscale modelling and medical informatics in biomedical engineering (SGABU)," [Online]. Available: http://sgabu.eu/. [Accessed 05 January 2023].

[3] I.I. Moraru, J.C. Schaff, B.M. Slepchenko, M.L. Blinov, F. Morgan, A...L.L. M. Lakshminarayana, Virtual cell modelling and simulation software environment, IET Syst. Biol. 2 (5) (2008) 352–362.

[4] P. Eastman, J. Swails, J.D. Chodera, R.T. McGibbon, Y. Zhao, K.A. Beauchamp, V. S. Pande, OpenMM 7: rapid development of high performance algorithms for molecular dynamics, PLoS Comput. Biol. 13 (7) (2017), e1005659.

[5] M.H. Swat, G.L. Thomas, J.M. Belmonte, A. Shirinifard, D. Hmeljak, J.A. Glazier, Multi-scale modeling of tissues using CompuCell3D, Methods Cell Biol. 110 (2012) 325–366.

[6] A. Seth, M. Sherman, J.A. Reinbolt, S.L. Delp, OpenSim: a musculoskeletal modeling and simulation framework for in silico investigations and exchange, Procedia IUTAM 2 (2011) 212–232.

[7] G.R. Mirams, C.J. Arthurs, M.O. Bernabeu, R. Bordas, J. Cooper, A. Corrias, D. J. Gavaghan, Chaste: an open source C++ library for computational physiology and biology, PLoS Comput. Biol. 9 (3) (2013), e1002970.

[8] P. Amstutz, M.R. Crusoe, N. Tijanić, B. Chapman, J. Chilton, M. Heuer, L. Stojanovic, Common workflow language, v1, Common Workflow Lang Working Group (2016) m9.

[9] J. Vivian, A.A. Rao, F.A. Nothaft, C. Ketchum, J. Armstrong, A. Novak, B..... Paten, Toil enables reproducible, open source, big biomedical data analyses, Nat. Biotechnol. 35 (4) (2017) 314–316.

[10] S. Seshadri, Angular: Up and running: Learning angular, Step by Step, O'Reilly Media, 2018.

[11] Plotly, 2022. [Online]. Available: https://plotly.com/. [Accessed 15 December 2022].

[12] E. Comission, "The EU's open science policy," 2022. [Online]. Available: https://research-and-innovation.ec.europa.eu/strategy/strategy-2020-2024/our-digital-future/open-science_en. [Accessed 23 January 2023].

[13] H. Kariem, M.I. Pastrama, S.I. Roohani-Esfahani, P. Pivonka, H. Zreiqat and C. Hellmich, "Micro-poro-elasticity of baghdadite-based bone tissue engineering scaffolds: a unifying approach based on ultrasonics, nanoindentation, and homogenization theory," in *Mater. Sci. Eng.: C*, 2015.

[14] O.A. Gkaintes, V.T. Potsika, V.S. Loukas, I. Gkiatas, E. Pakos, D.I. Fotiadis, Computational modelling of human femur after total hip arthroplasty, in: 44th Annual International Conference of the IEEE Engineering in Medicine & Biology Society (EMBC), IEEE, 2022, pp. 3947–3950.

[15] P.I. Tsompou, I.O. Andrikos, G.S. Karanasiou, A.I. Sakellarios, N. Tsigkas, V. I. Kigka, D.I. Fotiadis, Validation study of a novel method for the 3D reconstruction of coronary bifurcations, in: 2020 42nd Annual International Conference of the IEEE Engineering in Medicine & Biology Society (EMBC), IEEE, 2020, pp. 1576–1579.

[16] K.P. Exarchos, Y. Goletsis, D.I. Fotiadis, A multiscale and multiparametric approach for modeling the progression of oral cancer, BMC Med. Inform. Decis. Mak. 12 (1) (2012) 1–14.

[17] J. Barrasa-Fano, A. Shapeti, J. de Jong, A. Ranga, J.A. Sanz-Herrera, V.O. H, Advanced in silico validation framework for three-dimensional traction force microscopy and application to an in vitro model of sprouting angiogenesis, Acta Biomater. 126 (2021) 326–338.

[18] J. Barrasa-Fano, A. Shapeti, Á. Jorge-Peñas, M. Barzegari, J.A. Sanz-Herrera, H. V. Oosterwyck, TFMLAB: a MATLAB toolbox for 4D traction force microscopy, SoftwareX 15 (2021).

[19] Đ.G. Jakovljević, M.H. Yacoub, S. Schueler, G.A. MacGowan, L. Velicki, P. M. Seferovic, S. Hothi, B.-H. Tzeng, D.A. Brodie, E. Birks, L.-B. Tan, Left ventricular assist device as a bridge to recovery for patients with advanced heart failure, J. Am. Coll. Cardiol. 69 (15) (2017) 1924–1933.

[20] A. Vulović, N. Filipovic, Computational analysis of hip implant surfaces, J. Serbian Soc. Comput. Mech. 13 (2019) 109–119.

[21] K. Virijević, J. Grujić, M. Jovanovic, N. Kastratović, A. Mirić, D. Nikolić, M. Živanović, N. Filipović, Electrospun gelatin nanofibrous scaffolds – applications intissue engineering, in: 1st International Conference on Chemo and Bioinformatics, 2021, pp. 251–254.

[22] V. Vass, C. Morin, S. Scheiner, C. Hellmich, Review of "universal" rules governing bone composition, organization, and elasticity across organizational hierarchies, Multiscale Mechanobiol. Bone Remodel. Adaptat. 78 (2017) 175–229.

[23] F. Perez-Boerema, M. Barzegari, L. Geris, A flexible and easy-to-use open-source tool for designing functionally graded 3D porous structures, Virtual Phys. Prototyp. 17 (3) (2022) 682–699.

[24] T. Šušteršič, G.M. Simsek, G.G. Yapici, M. Nikolić, R. Vulović, N. Filipovic, N. E. Vrana, An In-Silico corrosion model for biomedical applications for coupling with in-vitro biocompatibility tests for estimation of Long-Term effects, Front. Bioeng. Biotechnol. 9 (2021).

[25] M. Anić, S. Savić, A. Milovanović, M. Milošević, B. Milićević, V. Simić, N. Filipović, Solution of fluid flow through the left heart ventricle, Appl. Eng. Lett. 5 (2020) 120–125.

[26] A. Dhanopia, M. Bhargava, Finite element analysis of human fractured femur bone implantation with PMMA thermoplastic prosthetic plate, Procedia Eng. 173 (2017) 1658–1665.

[27] A. Perez, A. Mahar, C. Negus, P. Newton, T. Impelluso, A computational evaluation of the effect of intramedullary nail material properties on the stabilization of simulated femoral shaft fractures, Med. Eng. Phys. 30 (6) (2008) 755–757.

[28] A. Vulovic, N. Filipovic, Calculation of femoral cortical bone elasticity modulus from computed tomography scans, in: 5th Serbian-Greek Symposium on Advanced Mechanics, Kragujevac, 2021.

[29] K. Chalernpon, P. Aroonjarattham, K. Aroonjarattham, Static and dynamic load on hip contact of hip prosthesis and Thai femoral bones, Int. J. Mech. Mechatron. Eng. 9 (3) (2015) 251–255.